hep-ph/0202110
CERN–TH/2002-027
UMN–TH–2042/02
TPI–MINN–02/02

# Constraining Supersymmetry

**John Ellis**[1], **Keith A. Olive**[2] and **Yudi Santoso**[2]

[1] *TH Division, CERN, Geneva, Switzerland*

[2] *Theoretical Physics Institute, University of Minnesota, Minneapolis, MN 55455, USA*

## Abstract

We review constraints on the minimal supersymmetric extension of the Standard Model (MSSM) coming from direct searches at accelerators such as LEP, indirect measurements such as $b \to s\gamma$ decay and the anomalous magnetic moment of the muon. The recently corrected sign of pole light-by-light scattering contributions to the latter is taken into account. We combine these constraints with those due to the cosmological density of stable supersymmetric relic particles. The possible indications on the supersymmetric mass scale provided by fine-tuning arguments are reviewed critically. We discuss briefly the prospects for future accelerator searches for supersymmetry.

*Invited Contribution to the New Journal of Physics Focus Issue on Supersymmetry*

CERN–TH/2002-027

# 1 Introduction

The avoidance of fine tuning has long been the primary motivation for supersymmetry at the TeV scale [1]. This issue is normally formulated in connection with the hierarchy problem: why/how is $m_W \ll m_P$, or equivalently why is $G_F \sim 1/m_W^2 \gg G_N = 1/m_P^2$, or equivalently why does the Coulomb potential in an atom dominate over the Newton potential, $e^2 \gg G_N m_p m_e \sim (m/m_P)^2$, where $m_{p,e}$ are the proton and electron masses? One might think naively that it would be sufficient to set $m_W \ll m_P$ by hand. However, radiative corrections tend to destroy this hierarchy. For example, one-loop diagrams generate

$$\delta m_W^2 = \mathcal{O}\left(\frac{\alpha}{\pi}\right) \Lambda^2 \gg m_W^2 \tag{1}$$

where $\Lambda$ is a cut-off representing the appearance of new physics, and the inequality in (1) applies if $\Lambda \sim 10^3$ TeV, and even more so if $\Lambda \sim m_{GUT} \sim 10^{16}$ GeV or $\sim m_P \sim 10^{19}$ GeV. If the radiative corrections to a physical quantity are much larger than its measured values, obtaining the latter requires strong cancellations, which in general require fine tuning of the bare input parameters. However, the necessary cancellations are natural in supersymmetry, where one has equal numbers of bosons $B$ and fermions $F$ with equal couplings, so that (1) is replaced by

$$\delta m_W^2 = \mathcal{O}\left(\frac{\alpha}{\pi}\right) |m_B^2 - m_F^2| \ . \tag{2}$$

The residual radiative correction is naturally small if

$$|m_B^2 - m_F^2| \lesssim 1 \text{ TeV}^2 \tag{3}$$

As we shall see later, cosmology also favours the mass range (3) for the lightest supersymmetric particle (LSP), if it is stable. In this case, the LSP would be an excellent candidate for astrophysical dark matter [2]. In the following the LSP is assumed to be a neutralino $\chi$, i.e., a mixture of the $\tilde{\gamma}, \tilde{H}$ and $\tilde{Z}$.

The minimal supersymmetric extension of the Standard Model (MSSM) has the same gauge interactions as the Standard Model, and similar Yukawa couplings. A key difference is the necessity of two Higgs doublets, in order to give masses to all the quarks and leptons, and to cancel triangle anomalies. This duplication is important for phenomenology: it means that there are five physical Higgs bosons, two charged $H^\pm$ and three neutral $h, H, A$. Their quartic self-interactions are determined by the gauge interactions, solving the vacuum instability problem mentioned above and limiting the possible mass of the lightest neutral Higgs boson. However, the doubling of the Higgs multiplets introduces two new parameters: $\tan\beta$, the ratio of Higgs vacuum expectation values and $\mu$, a parameter mixing the two Higgs doublets.

The MSSM predicts that there should appear a Higgs boson weighing $\lesssim 130$ GeV. Thus, fans of supersymmetry have been encouraged by the fact that the precision electroweak data favour [3] a relatively light Higgs boson with $m_H \simeq 115$ GeV, just above the exclusion unit provided by direct searches at LEP. They were even more encouraged by the possible sighting during the last days of LEP of a Higgs boson, with a preferred mass of 115.6 GeV [4].

If this were to be confirmed, it would suggest that the Standard Model breaks down at some relatively low energy $\lesssim 10^3$ TeV [5]. Above this scale the effective Higgs potential of the Standard Model becomes unstable as the quartic Higgs self-coupling is driven negative by radiative corrections due to the relatively heavy top quark [6]. This is not necessarily a disaster, and it is possible that the present electroweak vacuum might be metastable, provided that its lifetime is longer than the age of the Universe [7]. However, we would surely feel more secure if such an instability could be avoided by introducing suitable new physics below $10^3$ TeV. However, any new physics must be finely tuned, or the potential blows up instead [5], and this fine tuning also occurs naturally in supersymmetry. However, this argument is logically distinct from the previous hierarchy argument. There supersymmetry was motivated by the control of quadratic divergences, and here by the absence of logarithmic divergences.

Another experimental hint in favour of supersymmetry is provided by the LEP measurements of the gauge couplings, that are in very good agreement with supersymmetric GUTs [8], again if sparticles weigh $\sim 1$ TeV. This argument does not provide a strong constraint on the supersymmetry-breaking scale, particularly because there may be important threshold effects near the GUT scale, but it does favour qualitatively models with accessible sparticles.

A crucial ingredient in the MSSM is the soft supersymmetry breaking, in the form of scalar masses $m_0$, gaugino masses $m_{1/2}$ and trilinear couplings $A$ [9]. These are presumed to be inputs from physics at some high-energy scale, e.g., from some supergravity or superstring theory, which then evolve down to lower energy scale according to well-known renormalization-group equations. In the case of the Higgs multiplets, this renormalization can drive the effective mass-squared negative, triggering electroweak symmetry breaking [10]. It is often assumed that the $m_0$ are universal at the input scale [1], as are the $m_{1/2}$ and $A$ parameters. In this case the free parameters are

$$m_0, m_{1/2}, A \quad \text{and} \quad \tan\beta \ , \tag{4}$$

with $\mu$ being determined by the electroweak vacuum conditions, up to a sign. We refer to this scenario as the constrained MSSM (CMSSM).

# 2 Constraints on the MSSM

Important experimental constraints on the MSSM parameter space are provided by direct searches at LEP and the Tevatron collider, as seen in Fig. 1 in the case of the CMSSM. One of these is the limit $m_{\chi^\pm} \gtrsim 103.5$ GeV provided by chargino searches at LEP [12], where the third significant figure depends on other CMSSM parameters. LEP has also provided lower limits on slepton masses, of which the strongest is $m_{\tilde{e}} \gtrsim 99$ GeV [13], again depending only sightly on the other CMSSM parameters, as long as $m_{\tilde{e}} - m_\chi \gtrsim 10$ GeV. The most important

[1] Universality between the squarks and sleptons of different generations is motivated by upper limits on flavour-changing neutral interactions [11], but universality between the soft masses of the $L, E^c, Q^c, D^c$ and $U^c$ is not so well motivated.

constraints on the $u, d, s, c, b$ squarks and gluinos are provided by the Tevatron collider: for equal masses $m_{\tilde{q}} = m_{\tilde{g}} \gtrsim 300$ GeV. In the case of the $\tilde{t}$, LEP provides the most stringent limit when $m_{\tilde{t}} - m_\chi$ is small, and the Tevatron for larger $m_{\tilde{t}} - m_\chi$ [12].

Another important constraint is provided by the LEP lower limit on the Higgs mass: $m_H > 114.1$ GeV [4]. This holds in the Standard Model, for the lightest Higgs boson $h$ in the general MSSM for $\tan\beta \lesssim 8$, and almost always in the CMSSM for all $\tan\beta$, at least as long as CP is conserved [2]. Since $m_h$ is sensitive to sparticle masses, particularly $m_{\tilde{t}}$, via loop corrections:

$$\delta m_h^2 \propto \frac{m_t^4}{m_W^2} \ln\left(\frac{m_{\tilde{t}}^2}{m_t^2}\right) + \dots \tag{5}$$

the Higgs limit also imposes important constraints on the CMSSM parameters, principally $m_{1/2}$ as seen in Fig. 1. The constraints are evaluated using `FeynHiggs` [17], which is estimated to have a residual uncertainty of a couple of GeV in $m_h$.

Also shown in Fig. 1 is the constraint imposed by measurements of $b \to s\gamma$ [15]. These agree with the Standard Model, and therefore provide bounds on MSSM particles, such as the chargino and charged Higgs masses, in particular. Typically, the $b \to s\gamma$ constraint is more important for $\mu < 0$, as seen in Fig. 1a and c, but it is also relevant for $\mu > 0$, particularly when $\tan\beta$ is large as seen in Fig. 1d.

The final experimental constraint we consider is that due to the measurement of the anamolous magnetic moment of the muon. The BNL E821 experiment reported last year a new measurement of $a_\mu \equiv \frac{1}{2}(g_\mu - 2)$ which deviated by 2.6 standard deviations from the best Standard Model prediction available at that time [18]. The largest contribution to the errors in the comparison with theory was thought to be the statistical error of the experiment, which will soon be significantly reduced, as many more data have already been recorded. However, it has recently been realized that the sign of the most important pseudoscalar-meson pole part of the light-by-light scattering contribution [19] to the Standard Model prediction should be reversed, which reduces the apparent experimental discrepancy to about 1.6 standard deviations. The next-largest error is thought to be that due to strong-interaction uncertainties in the Standard Model prediction, for which recent estimates converge to about $7\times10^{-10}$ [20].

As many authors have pointed out [21], a discrepancy between theory and the BNL experiment could well be explained by supersymmetry. As seen in Fig. 1, this is particularly easy if $\mu > 0$. With the change in sign of the meson-pole contributions to light-by-light scattering, good consistency is also possible for $\mu < 0$ so long as either $m_{1/2}$ or $m_0$ are taken sufficiently large. We show in Fig. 1 as medium (pink) shaded the new $2\,\sigma$ allowed region: $-6 < \delta a_\mu \times 10^{10} < 58$.

The new regions preferred by the $g-2$ experimental data shown in Fig. 1 differ considerably from the older ones [21] which were based on the range $11 < \delta a_\mu \times 10^{10} < 75$. First of all, the older bound completely excluded $\mu < 0$ at the $2\,\sigma$ level. As one can see this is no longer treu. $\mu < 0$ is allowed so long as either (or both) $m_{1/2}$ and $m_0$ are large.

[2] The lower bound on the lightest MSSM Higgs boson may be relaxed significantly if CP violation feeds into the MSSM Higgs sector [16].

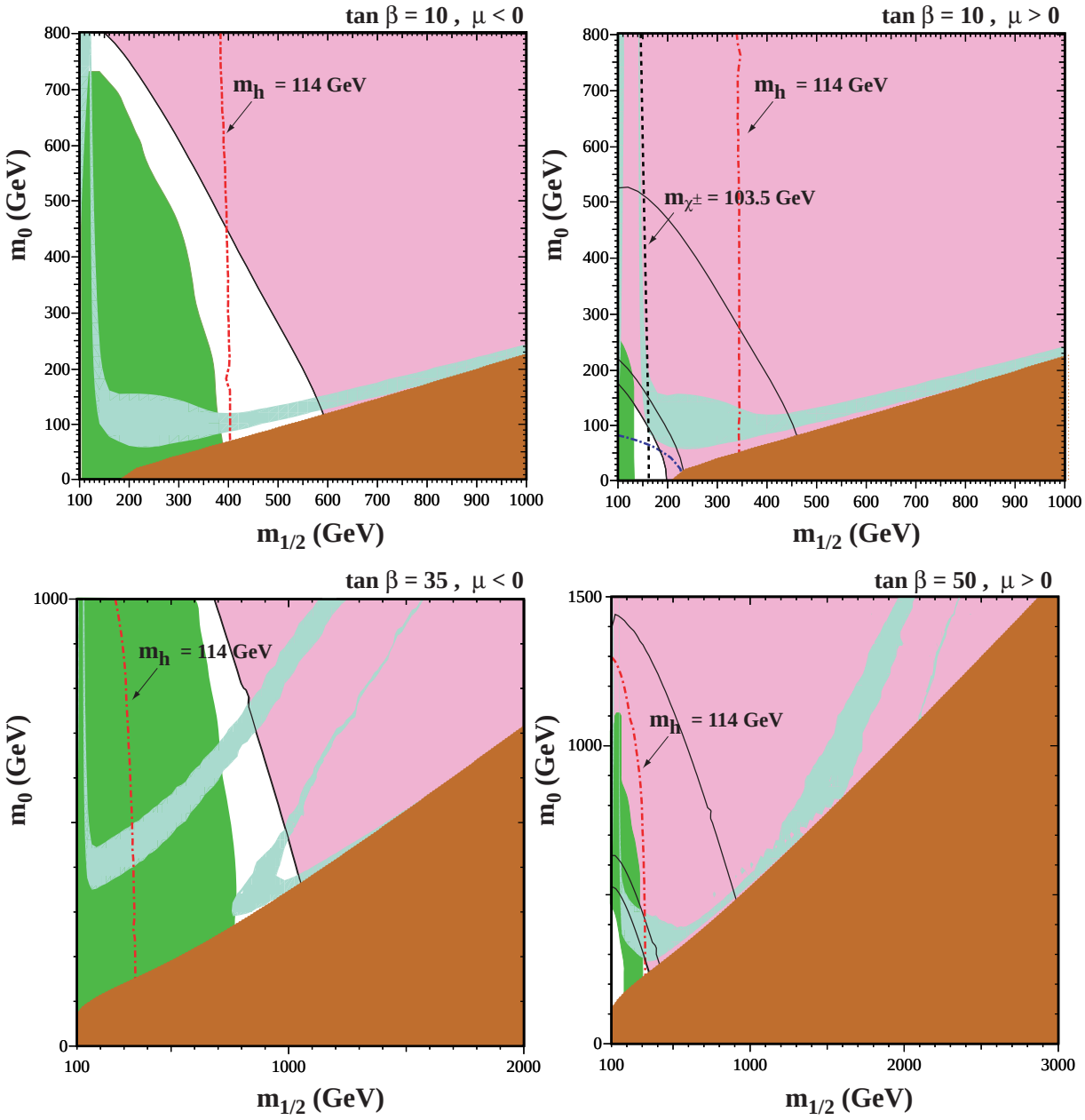


Figure 1: *Compilations of phenomenological constraints on the CMSSM for (a)* $\tan\beta = 10, \mu < 0$*, (b)* $\tan\beta = 10, \mu > 0$*, (c)* $\tan\beta = 35, \mu < 0$ *and (d)* $\tan\beta = 50, \mu > 0$*, assuming* $A_0 = 0, m_t = 175$ *GeV and* $m_b(m_b)^{\overline{MS}}_{SM} = 4.25$ *GeV [14]. The near-vertical lines are the LEP limits* $m_{\chi^\pm} = 103.5$ *GeV (dashed and black) [12], shown in (b) only, and* $m_h = 114.1$ *GeV (dotted and red) [4]. Also, in the lower left corner of (b), we show the* $m_{\tilde{e}} = 99$ *GeV contour [13]. In the dark (brick red) shaded regions, the LSP is the charged* $\tilde{\tau}_1$*, so this region is excluded. The light (turquoise) shaded areas are the cosmologically preferred regions with* $0.1 \leq \Omega_\chi h^2 \leq 0.3$ *[14]. The medium (dark green) shaded regions that are most prominent in panels (a) and (c) are excluded by* $b \to s\gamma$ *[15]. The shaded (pink) regions in the upper right regions delineate the* $\pm 2\,\sigma$ *ranges of* $g_\mu - 2$*. For* $\mu > 0$*, the* $\pm 1\,\sigma$ *contours are also shown as solid black lines.*

Thus for $\mu < 0$, one is forced into either the $\chi - \tilde{\tau}$ coannihilation region or the funnel region produced by the s-channel annihilatn via the heavy Higgses $H$ and $A$. Second, whereas the older limits produced definite upper bounds on the sparticle masses (which were accept with delight to future collider builders), the new bounds which are consistent with $a_m u = 0$, allow arbitrarily high sparticle masses. Now only the very low mass corner of the $m_{1/2} - m_0$ plane is excluded.

Fig. 1 also displays the regions where the supersymmetric relic density $\rho_\chi = \Omega_\chi \rho_{critical}$ falls within the preferred range

$$0.1 < \Omega_\chi h^2 < 0.3 \tag{6}$$

The upper limit is rigorous, since astrophysics and cosmology tell us that the total matter density $\Omega_m \lesssim 0.4$, and the Hubble expansion rate $h \sim 1/\sqrt{2}$ to within about 10 % (in units of 100 km/s/Mpc). On the other hand, the lower limit in (6) is optional, since there could be other important contributions to the overall matter density.

As is seen in Fig. 1, there are generic regions of the CMSSM parameter space where the relic density falls within the preferred range (6). What goes into the calculation of the relic density? It is controlled by the annihilation cross section [2]:

$$\rho_\chi = m_\chi n_\chi \,, \quad n_\chi \sim \frac{1}{\sigma_{ann}(\chi\chi \to \ldots)} \,, \tag{7}$$

where the typical annihilation cross section $\sigma_{ann} \sim 1/m_\chi^2$. For this reason, the relic density typically increases with the relic mass, and this combined with the upper bound in (6) then leads to the common expectation that $m_\chi \lesssim$ O(200) GeV.

However, there are various ways in which the generic upper bound on $m_\chi$ can be increased along filaments in the $(m_{1/2}, m_0)$ plane. For example, if the next-to-lightest sparticle (NLSP) is not much heavier than $\chi$: $\Delta m/m_\chi \lesssim 0.1$, the relic density may be suppressed by coannihilation: $\sigma(\chi$+NLSP$\to \ldots)$ [22]. In this way, the allowed CMSSM region may acquire a 'tail' extending to larger sparticle masses. An example of this possibility is the case where the NLSP is the lighter stau: $\tilde{\tau}_1$ and $m_{\tilde{\tau}_1} \sim m_\chi$, as seen in Figs. 1(a) and (b) and extended to larger $m_{1/2}$ in Fig. 2(a) [23]. Another example is coannihilation when the NLSP is the lighter stop [24]: $\tilde{t}_1$ and $m_{\tilde{t}_1} \sim m_\chi$, which may be important in the general MSSM or in the CMSSM when $A$ is large, as seen in Fig. 2(b) [25]. In the cases studied, the upper limit on $m_\chi$ is not affected by stop coannihilation. Another mechanism for extending the allowed CMSSM region to large $m_\chi$ is rapid annihilation via a direct-channel pole when $m_\chi \sim \frac{1}{2} m_{Higgs,Z}$ [26, 14]. This may yield a 'funnel' extending to large $m_{1/2}$ and $m_0$ at large $\tan\beta$, as seen in panels (c) and (d) of Fig. 1 [14]. Yet another allowed region at large $m_{1/2}$ and $m_0$ is the 'focus-point' region [27], which is adjacent to the boundary of the region where electroweak symmetry breaking is possible, as seen in Fig. 3.

# 3 Fine Tuning

The filaments extending the preferred CMSSM parameter space are clearly exceptional, in some sense, so it is important to understand the sensitivity of the relic density to input

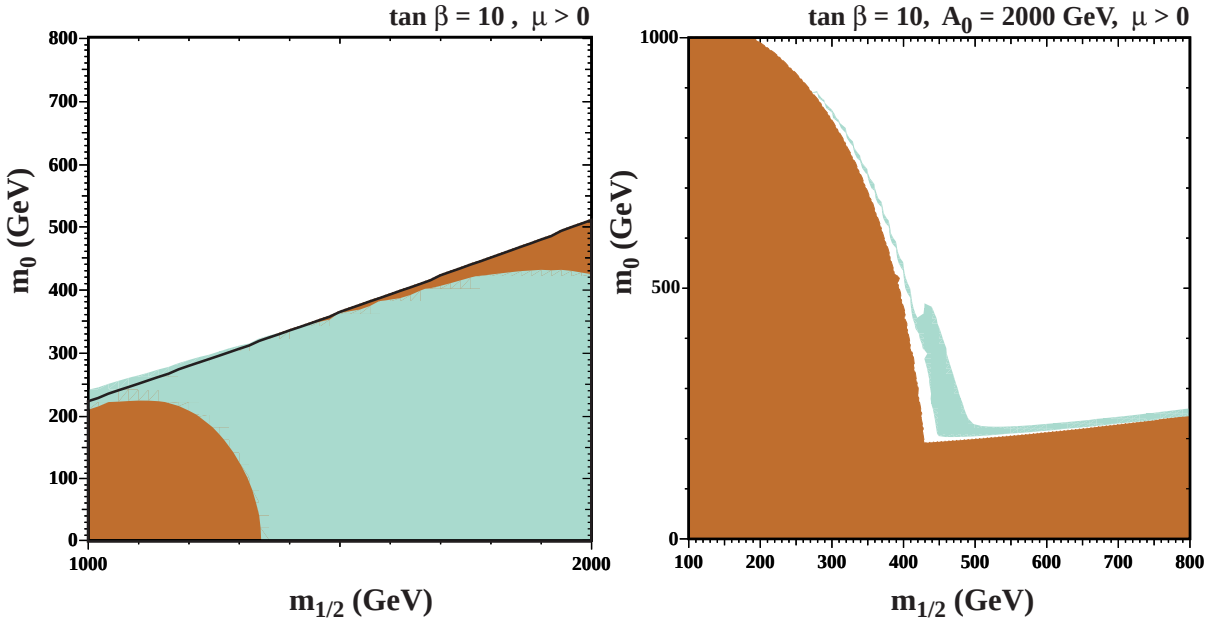


Figure 2: *(a) The large-$m_{1/2}$ 'tail' of the $\chi - \tilde{\tau}_1$ coannihilation region for* $\tan\beta = 10$, $A = 0$ *and* $\mu < 0$ *[23], superimposed on the disallowed dark (brick red) shaded region where* $m_{\tilde{\tau}_1} < m_\chi$, *and (b) the* $\chi - \tilde{t}_1$ *coannihilation region for* $\tan\beta = 10$, $A = 2000$ *GeV and* $\mu > 0$ *[25], exhibiting a large-$m_0$ 'tail'.*

parameters, unknown higher-order effects, etc. One proposal is the relic-density fine-tuning measure [28]

$$\Delta^\Omega \equiv \sqrt{\sum_i \left(\frac{\partial \ln(\Omega_\chi h^2)}{\partial \ln a_i}\right)^2} \tag{8}$$

where the sum runs over the input parameters, which might include (relatively) poorly-known Standard Model quantities such as $m_t$ and $m_b$, as well as the CMSSM parameters $m_0, m_{1/2}$, etc. As seen in Fig. 4, the sensitivity $\Delta^\Omega$ (8) is relatively small in the 'bulk' region at low $m_{1/2}$, $m_0$, and $\tan\beta$. However, it is somewhat higher in the $\chi - \tilde{\tau}_1$ coannihilation 'tail', and at large $\tan\beta$ in general. The sensitivity measure $\Delta^\Omega$ (8) is particularly high in the rapid-annihilation 'funnel' and in the 'focus-point' region. This explains why published relic-density calculations may differ in these regions [29], whereas they agree well when $\Delta^\Omega$ is small: differences may arise because of small differences in the treatments of the inputs.

It is important to note that the relic-density fine-tuning measure (8) is distinct from the traditional measure of the fine-tuning of the electroweak scale [30]:

$$\Delta = \sqrt{\sum_i {\Delta_i}^2}, \quad \Delta_i \equiv \frac{\partial \ln m_W}{\partial \ln a_i} \tag{9}$$

Sample contours of the electroweak fine-tuning measure are shown (9) are shown in Figs. 5. This electroweak fine tuning is logically different from the cosmological fine tuning, and values of $\Delta$ are not necessarily related to values of $\Delta^\Omega$, as is apparent when comparing the contours in Figs. 4 and 5. Electroweak fine-tuning is sometimes used as a criterion for

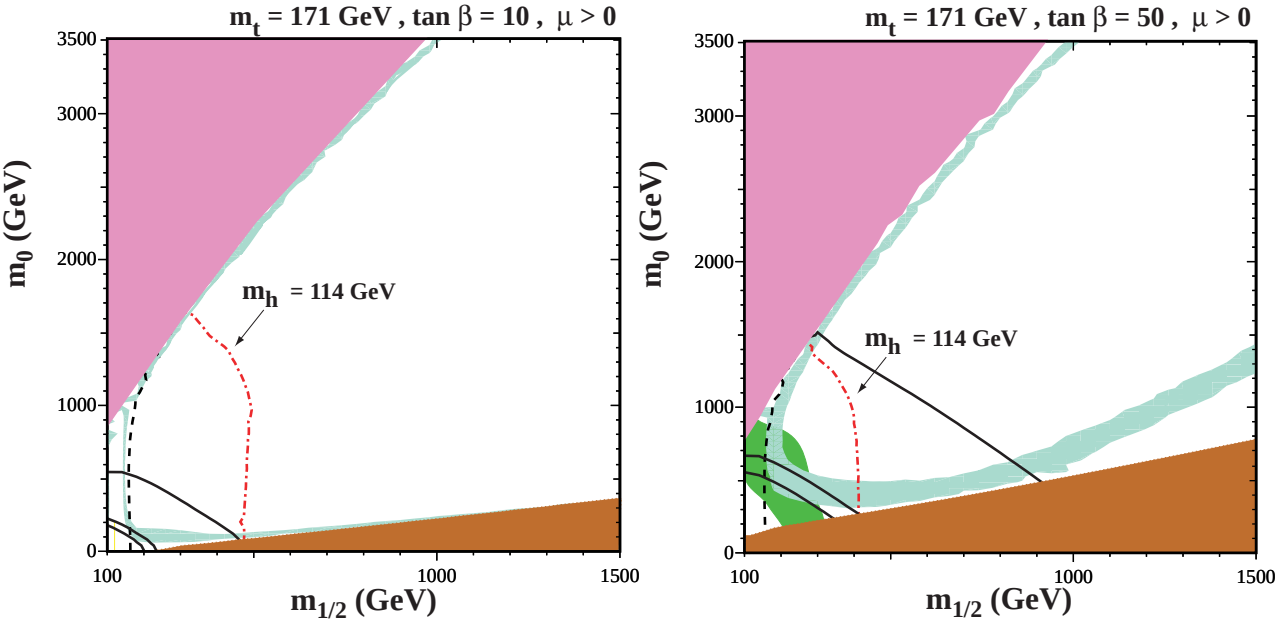


Figure 3: *An expanded view of the $m_{1/2} - m_0$ parameter plane showing the focus-point regions [27] at large $m_0$ for (a) tan$\beta = 10$, and (b) $\tan\beta = 50$. In the shaded (mauve) region in the upper left corner, there are no solutions with proper electroweak symmetry breaking, so these are excluded in the CMSSM. Note that we have chosen $m_t = 171$ GeV, in which case the focus-point region is at lower $m_0$ than when $m_t = 175$ GeV, as assumed in the other figures. The position of this region is very sensitive to $m_t$. The black contours (both dashed and solid) are as in Fig. 1, the we do not shade the preferred $g - 2$ region.*

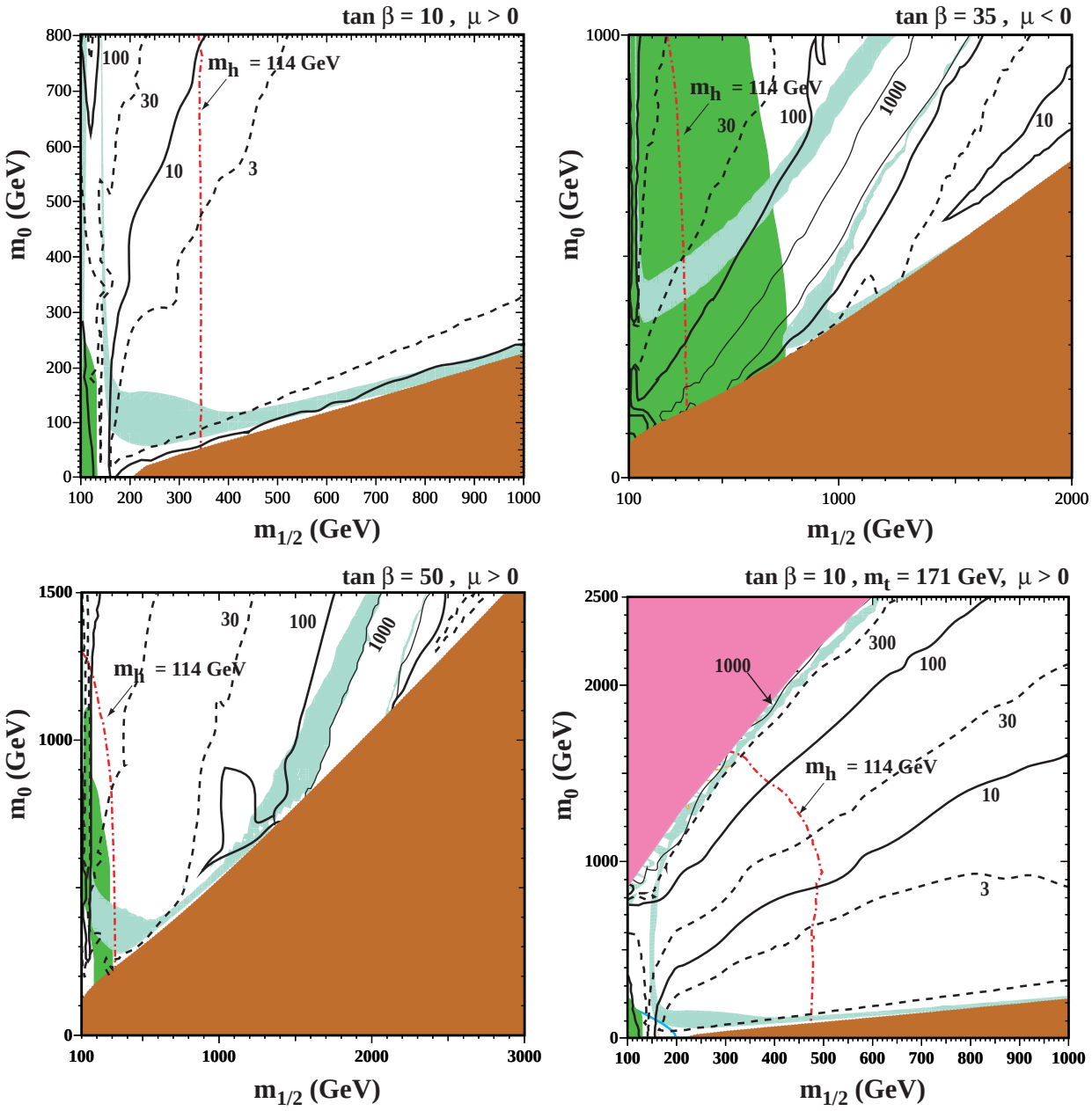


Figure 4: *Contours of the total sensitivity* $\Delta^{\Omega}$ *(8) of the relic density in the* $(m_{1/2}, m_0)$ *planes for (a)* $\tan\beta = 10, \mu > 0, m_t = 175$ *GeV, (b)* $\tan\beta = 35, \mu < 0, m_t = 175$ *GeV, (c)* $\tan\beta = 50, \mu > 0, m_t = 175$ *GeV, and (d)* $\tan\beta = 10, \mu > 0, m_t = 171$ *GeV, all for* $A_0 = 0$. *The light (turquoise) shaded areas are the cosmologically preferred regions with* $0.1 \leq \Omega_\chi h^2 \leq 0.3$. *In the dark (brick red) shaded regions, the LSP is the charged* $\tilde{\tau}_1$, *so these regions are excluded. In panel (d), the medium shaded (mauve) region is excluded by the electroweak vacuum conditions.*

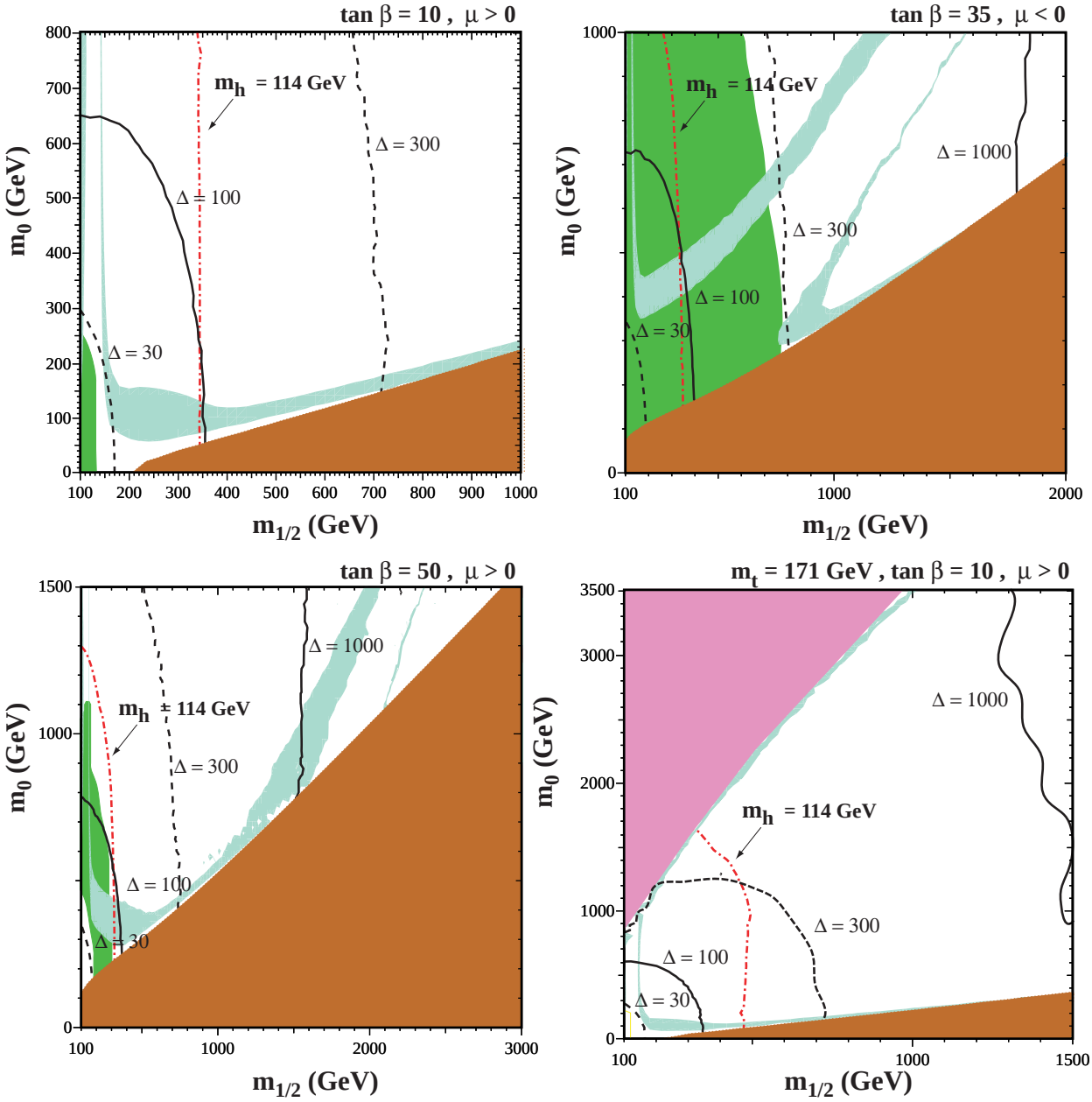


Figure 5: *Contours of the electroweak fine-tuning measure* $\Delta$ *(9) in the* $(m_{1/2}, m_0)$ *planes for (a)* $\tan\beta = 10, \mu > 0, m_t = 175$ *GeV, (b)* $\tan\beta = 35, \mu < 0, m_t = 175$ *GeV, (c)* $\tan\beta = 50, \mu > 0, m_t = 175$ *GeV, and (d)* $\tan\beta = 10, \mu > 0, m_t = 171$ *GeV, all for* $A_0 = 0$. *The light (turquoise) shaded areas are the cosmologically preferred regions with* $0.1 \leq \Omega_\chi h^2 \leq 0.3$. *In the dark (brick red) shaded regions, the LSP is the charged* $\tilde{\tau}_1$, *so this region is excluded. In panel (d), the medium shaded (mauve) region is excluded by the electroweak vacuum conditions.*

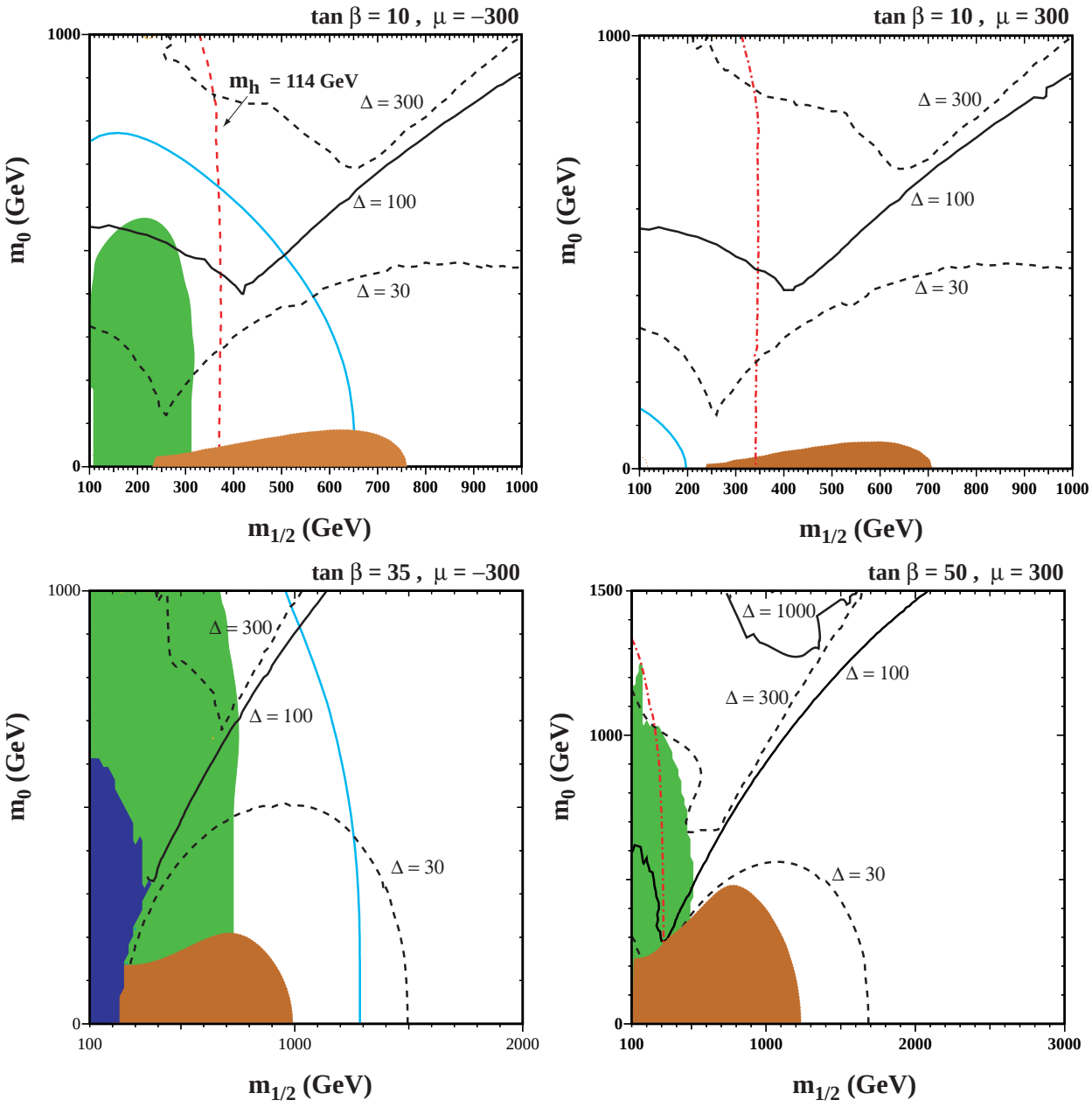


Figure 6: *Contours of the electroweak fine-tuning parameter* $\Delta$ *(9) for non-universal Higgs masses, in the* $(m_{1/2}, m_0)$ *planes for (a)* $\tan\beta = 10, \mu = -300$ *GeV, (b)* $\tan\beta = 10, \mu = 300$ *GeV, (c)* $\tan\beta = 35, \mu = -300$ *GeV, and (d)* $\tan\beta = 50, \mu = 300$ *GeV, all for* $m_t = 175$ *GeV,* $A_0 = 0$ *and* $m_A = 1$ *TeV. In the dark (brick red) shaded regions, the LSP is the charged* $\tilde{\tau}_1$*, so this region is excluded. In panel (c), the very dark shaded (dark blue) region is excluded by the electroweak vacuum conditions. The solid (turquoise) curve shows the* $2\,\sigma$ $g-2$ *bound.*

restricting the CMSSM parameters. However, the interpretation of $\Delta$ (9) is unclear. How large a value of $\Delta$ is tolerable? Different physicists may well have different pain thresholds. Moreover, correlations between input parameters may reduce its value in specific models.

Note that, the regions allowed by the different constraints can be very different from those in the CMSSM when we relax some of the CMSSM assumptions, e.g. the universality between the input Higgs masses and those of the squarks and sleptons, a subject too broad for complete study in this paper. As an exercise, we display in Fig. 6 the electroweak fine-tuning contours in the Non Universal Higgs Mass model (NUHM), where the soft breaking mass terms for the Higgs are not set to equal to $m_0$, but are derived from the electroweak symmetry breaking condition with two additional free parameters $m_A$ and $\mu$.

# 4 Prospects for Observing Supersymmetry at Accelerators

As an aid to the assessment of the prospects for detecting sparticles at different accelerators, benchmark sets of supersymmetric parameters have often been found useful [31], since they provide a focus for concentrated discussion. A set of proposed post-LEP benchmark scenarios in the CMSSM [32] are illustrated schematically in Fig. 7. They take into account the direct searches for sparticles and Higgs bosons, $b \to s\gamma$ and the preferred cosmological density range (6). About a half of the proposed benchmark points are consistent with $g_\mu - 2$ at the $2\,\sigma$ level, but this was not imposed as an absolute requirement.

The proposed points were chosen not to provide an 'unbiased' statistical sampling of the CMSSM parameter space, whatever that means in the absence of a plausible *a priori* measure, but rather are intended to illustrate the different possibilities that are still allowed by the present constraints [32] [3]. Five of the chosen points are in the 'bulk' region at small $m_{1/2}$ and $m_0$, four are spread along the coannihilation 'tail' at larger $m_{1/2}$ for various values of $\tan\beta$, two are in the 'focus-point' region at large $m_0$, and two are in rapid-annihilation 'funnels' at large $m_{1/2}$ and $m_0$. The proposed points range over the allowed values of $\tan\beta$ between 5 and 50. Most of them have $\mu > 0$, as favoured by $g_\mu - 2$, but there are two points with $\mu < 0$. All but one point are consistent with the revised value of $a_\mu$.

Various derived quantities in these supersymmetric benchmark scenarios, including the relic density, $g_\mu - 2, b \to s\gamma$, electroweak fine-tuning $\Delta$ and the relic-density sensitivity $\Delta^\Omega$, are given in [32]. These enable the reader to see at a glance which models would be excluded by which refinement of the experimental value of $g_\mu - 2$. Likewise, if you find some amount of fine-tuning uncomfortably large, then you are free to discard the corresponding models.

The LHC collaborations have analyzed their reach for sparticle detection in both generic studies and specific benchmark scenarios proposed previously [33]. Based on these studies, Fig. 8 displays estimates of how many different sparticles may be seen at the LHC in each of the newly-proposed benchmark scenarios [32]. The lightest Higgs boson is always found, and squarks and gluinos are usually found, though there are some scenarios where no sparticles

[3] This study is restricted to $A = 0$, for which $\tilde{t}_1 - \chi$ coannihilation is less important, so this effect has not influenced the selection of benchmark points.

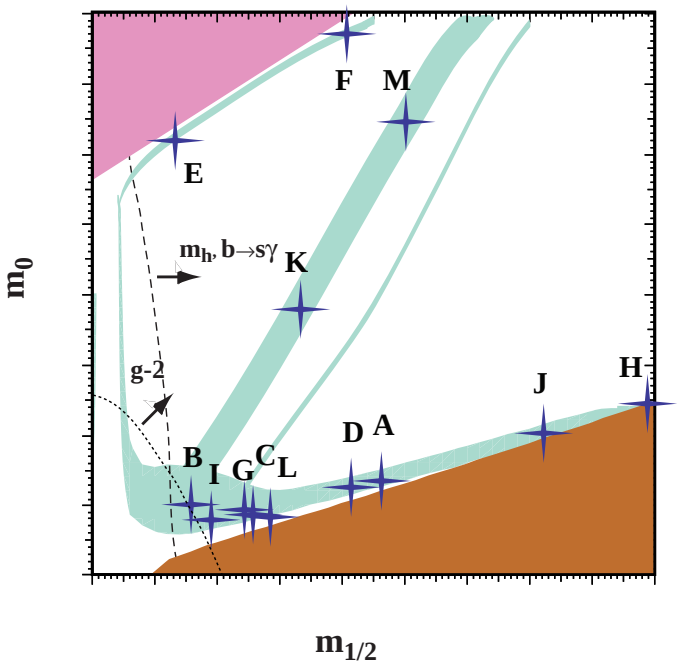


Figure 7: *Schematic overview of the CMSSM benchmark points proposed in [32]. They were chosen to be compatible with the indicated experimental constraints, as well as have a relic density in the preferred range (6). The points are intended to illustrate the range of available possibilities. The labels correspond to the approximate positions of the benchmark points in the* $(m_{1/2}, m_0)$ *plane.*

are found at the LHC. The LHC often misses heavier weakly-interacting sparticles such as charginos, neutralinos, sleptons and the other Higgs bosons.

It was initially thought that the discovery of supersymmetry at the LHC was 'guaranteed' if the BNL measurement $g_\mu - 2$ was within $2\,\sigma$ of the true value, but this is no longer the case with the new sign of the pole contributions to light-by-light scattering. This is the case, in particular, because arbitrarily large values of $m_{1/2}$ and $m_0$ are now compatible with the data at the $2\,\sigma$ level [34].

The physics capabilities of linear $e^+e^-$ colliders are amply documented in various design studies [35]. Not only is the lightest MSSM Higgs boson observed, but its major decay modes can be measured with high accuracy. Moreover, if sparticles are light enough to be produced, their masses and other properties can be measured very precisely, enabling models of supersymmetry breaking to be tested [38].

As seen in Fig. 8, the sparticles visible at an $e^+e^-$ collider largely complement those visible at the LHC [32, 34]. In most of benchmark scenarios proposed, a 1-TeV linear collider would be able to discover and measure precisely several weakly-interacting sparticles that are invisible or difficult to detect at the LHC. However, there are some benchmark scenarios where the linear collider (as well as the LHC) fails to discover supersymmetry. Only a linear collider with a higher centre-of-mass energy appears sure to cover all the allowed CMSSM parameter space, as seen in the lower panels of Fig. 8, which illustrate the physics reach of a higher-energy lepton collider, such as CLIC [36] or a multi-TeV muon collider [37].

# 5 Prospects for Other Experiments

## 5.1 Detection of Cold Dark Matter

Fig. 9 shows rates for the elastic spin-independent scattering of supersymmetric relics [39], including the projected sensitivities for CDMS II [40] and CRESST [41] (solid) and GENIUS [42] (dashed). Also shown are the cross sections calculated in the proposed benchmark scenarios discussed in the previous section, which are considerably below the DAMA [43] range ($10^{-5} - 10^{-6}$ pb), but may be within reach of future projects. Indirect searches for supersymmetric dark matter via the products of annihilations in the galactic halo or inside the Sun also have prospects in some of the benchmark scenarios [39].

## 5.2 Proton Decay

This could be within reach, with $\tau(p \to e^+\pi^0)$ via a dimension-six operator possibly $\sim 10^{35}y$ if $m_{GUT} \sim 10^{16}$ GeV as expected in a minimal supersymmetric GUT. Such a model also suggests that $\tau(p \to \bar{\nu}K^+) < 10^{32}y$ via dimension-five operators [45], unless measures are taken to suppress them [46]. This provides motivation for a next-generation megaton experiment that could detect proton decay as well as explore new horizons in neutrino physics [47].

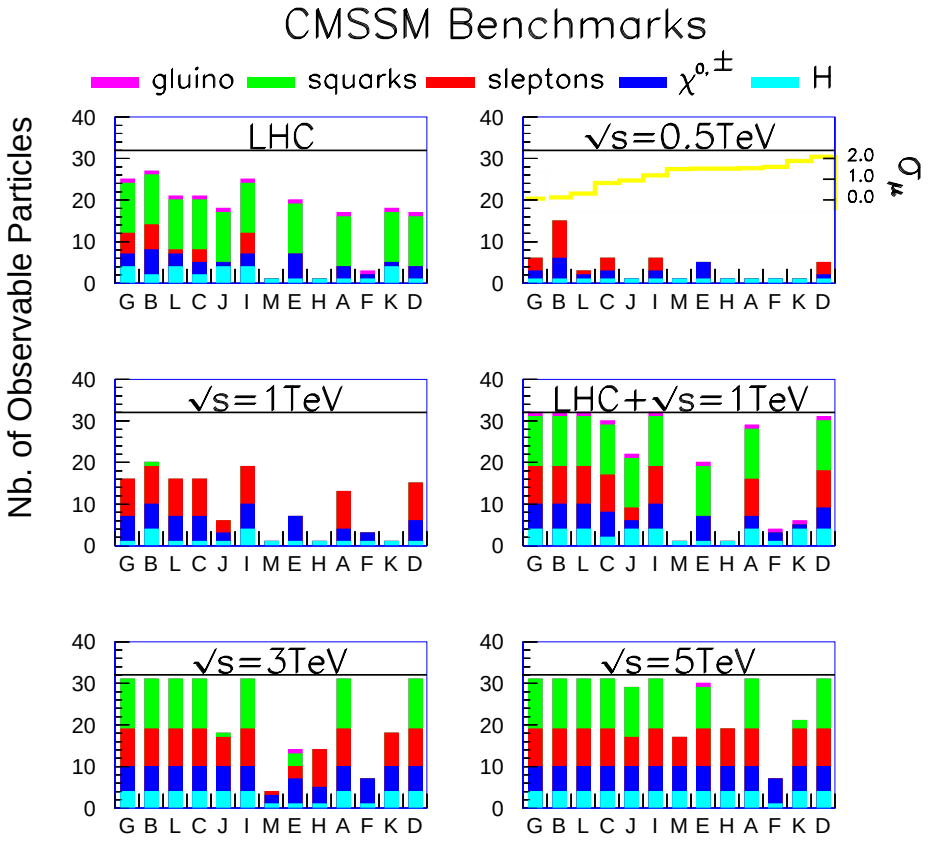


Figure 8: *Summary of the prospective sensitivities of the LHC and linear colliders at different* $\sqrt{s}$ *energies to CMSSM particle production in the proposed benchmark scenarios G, B, ..., which are ordered by their distance from the central value of* $g_\mu - 2$*, as indicated by the pale (yellow) line in the second panel. We see clearly the complementarity between an* $e^+e^-$ *collider [35, 36] (or* $\mu^+\mu^-$ *collider [37]) and the LHC in the TeV range of energies [32], with the former excelling for non-strongly-interacting particles, and the LHC for strongly-interacting sparticles and their cascade decays. CLIC [36] provides unparallelled physics reach for non-strongly-interacting sparticles, extending beyond the TeV scale. We recall that mass and coupling measurements at* $e^+e^-$ *colliders are usually much cleaner and more precise than at hadron-hadron colliders such as the LHC. Note, in particular, that it is not known how to distinguish the light squark flavours at the LHC.*

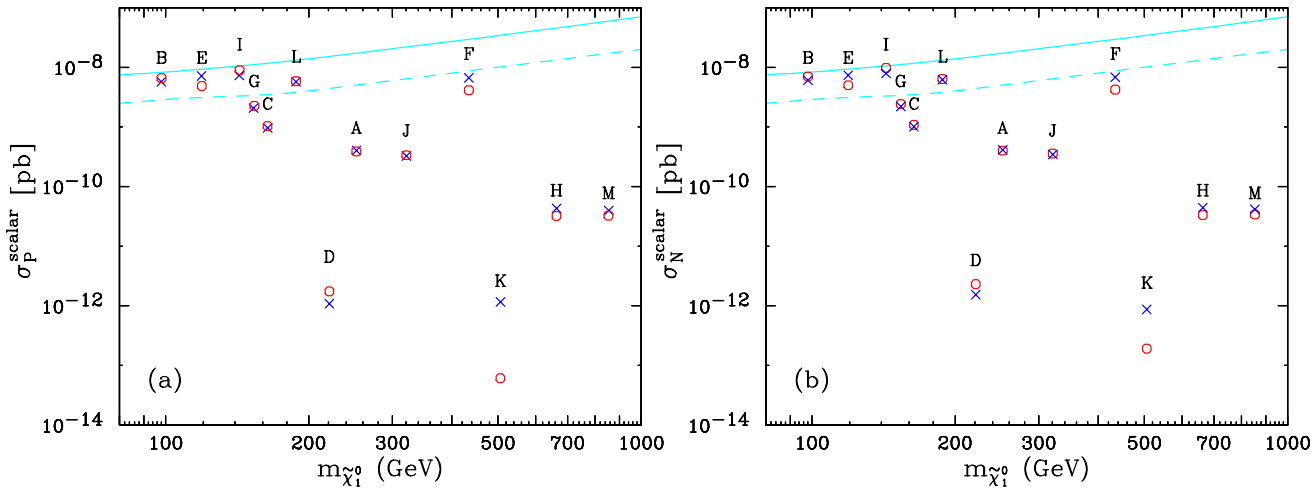


Figure 9: *Elastic spin-independent scattering of supersymmetric relics on (a) protons and (b) neutrons calculated in benchmark scenarios [39], compared with the projected sensitivities for CDMS II [40] and CRESST [41] (solid) and GENIUS [42] (dashed). The predictions of our code (blue crosses) and* `Neutdriver`*[44] (red circles) for neutralino-nucleon scattering are compared. The labels A, B, ...,L correspond to the benchmark points as shown in Fig. 7.*

# 6 Conclusions

We have compiled in this short review the various experimental constraints on the MSSM, particularly in its constrained CMSSM version. These have been compared and combined with the cosmological constraint on the relic dark matter density. As we have shown, there is good overall compatibility between these various constraints. To exemplify the possible types of supersymmetric phenomenology compatible with all these constraints, a set of benchmark scenarios have been proposed.

We have discussed the fine-tuning of parameters required for supersymmetry to have escaped detection so far. There are regions of parameter space where the neutralino relic density is rather sensitive to the exact values of the input parameters, and to the details of the calculations based on them. However, there are generic domains of parameter space where supersymmetric dark matter is quite natural. The fine-tuning price of the electroweak supersymmetry-breaking scale has been increased by the experimental constraints due to LEP, in particular, but its significance remains debatable.

As illustrated by these benchmark scenarios, future colliders such as the LHC and a TeV-scale linear $e^+e^-$ collider have good prospects of discovering supersymmetry and making detailed measurements. There are also significant prospects for discovering supersymmetry via searches for cold dark matter particles, and searches for proton decay also have interesting prospects in supersymmetric GUT models.

One may be disappointed that supersymmetry has not already been discovered, but one should not be disheartened. Most of the energy range where supersymmetry is expected to appear has yet to be explored. Future accelerators will be able to complete the search for supersymmetry, but they may be scooped by non-accelerator experiments. In a few years'

time, we expect to be writing about the discovery of supersymmetry, not just constraints on its existence.

# References


[1] L. Maiani, *Proceedings of the 1979 Gif-sur-Yvette Summer School On Particle Physics*, 1; G. 't Hooft, in *Recent Developments in Gauge Theories, Proceedings of the Nato Advanced Study Institute, Cargese, 1979*, eds. G. 't Hooft *et al.*, (Plenum Press, NY, 1980); E. Witten, Phys. Lett. B **105** (1981) 267.

[2] J. Ellis, J.S. Hagelin, D.V. Nanopoulos, K.A. Olive and M. Srednicki, Nucl. Phys. B **238** (1984) 453; see also H. Goldberg, Phys. Rev. Lett. **50** (1983) 1419.

[3] LEP Electroweak Working Group, `http://lepewwg.web.cern.ch/LEPEWWG/Welcome.html`.

[4] LEP Higgs Working Group for Higgs boson searches, OPAL Collaboration, ALEPH Collaboration, DELPHI Collaboration and L3 Collaboration, *Search for the Standard Model Higgs Boson at LEP*, ALEPH-2001-066, DELPHI-2001-113, CERN-L3-NOTE-2699, OPAL-PN-479, LHWG-NOTE-2001-03, CERN-EP/2001-055, arXiv:hep-ex/0107029; *Searches for the neutral Higgs bosons of the MSSM: Preliminary combined results using LEP data collected at energies up to 209 GeV*, LHWG-NOTE-2001-04, ALEPH-2001-057, DELPHI-2001-114, L3-NOTE-2700, OPAL-TN-699, arXiv:hep-ex/0107030.

[5] J. R. Ellis and D. Ross, Phys. Lett. B **506** (2001) 331 [arXiv:hep-ph/0012067].

[6] For a review, see: T. Hambye and K. Riesselmann, arXiv:hep-ph/9708416.

[7] G. Isidori, G. Ridolfi and A. Strumia, Nucl. Phys. B **609** (2001) 387 [arXiv:hep-ph/0104016].

[8] J. Ellis, S. Kelley and D. V. Nanopoulos, Phys. Lett. B **260** (1991) 131; U. Amaldi, W. de Boer and H. Furstenau, Phys. Lett. B **260** (1991) 447; C. Giunti, C. W. Kim and U. W. Lee, Mod. Phys. Lett. A **6** (1991) 1745.

[9] S. Dimopoulos and H. Georgi, Nucl. Phys. B **193** (1981) 150; N. Sakai, Z. Phys. C **11** (1981) 153.

[10] K. Inoue, A. Kakuto, H. Komatsu and S. Takeshita, Prog. Theor. Phys. **68** (1982) 927 [Erratum-ibid. **70** (1982) 330]; L.E. Ibáñez and G.G. Ross, Phys. Lett. B **110** (1982) 215; L.E. Ibáñez, Phys. Lett. B **118** (1982) 73; J. Ellis, D.V. Nanopoulos and K. Tamvakis, Phys. Lett. B **121** (1983) 123; J. Ellis, J. Hagelin, D.V. Nanopoulos and K. Tamvakis, Phys. Lett. B **125** (1983) 275; L. Alvarez-Gaumé, J. Polchinski, and M. Wise, Nucl. Phys. B **221** (1983) 495.

[11] J. R. Ellis and D. V. Nanopoulos, Phys. Lett. B **110** (1982) 44; R. Barbieri and R. Gatto, Phys. Lett. B **110** (1982) 211.

[12] Joint LEP 2 Supersymmetry Working Group, *Combined LEP Chargino Results, up to 208 GeV*, `http://lepsusy.web.cern.ch/lepsusy/www/inos_moriond01/charginos_pub.html`.

[13] Joint LEP 2 Supersymmetry Working Group, *Combined LEP Selectron/Smuon/Stau Results, 183-208 GeV*, `http://alephwww.cern.ch/~ganis/SUSYWG/SLEP/sleptons_2k01.html`.

[14] J. R. Ellis, T. Falk, G. Ganis, K. A. Olive and M. Srednicki, Phys. Lett. B **510** (2001) 236 [arXiv:hep-ph/0102098].

[15] M.S. Alam et al., [CLEO Collaboration], Phys. Rev. Lett. **74** (1995) 2885 as updated in S. Ahmed et al., CLEO CONF 99-10; BELLE Collaboration, BELLE-CONF-0003, contribution to the 30th International conference on High-Energy Physics, Osaka, 2000. See also K. Abe *et al.*, [Belle Collaboration], [arXiv:hep-ex/0107065]; L. Lista [BaBar Collaboration], [arXiv:hep-ex/0110010]; C. Degrassi, P. Gambino and G. F. Giudice, JHEP **0012** (2000) 009 [arXiv:hep-ph/0009337]; M. Carena, D. Garcia, U. Nierste and C. E. Wagner, Phys. Lett. B **499** (2001) 141 [arXiv:hep-ph/0010003].

[16] M. Carena, J. R. Ellis, A. Pilaftsis and C. E. Wagner, Nucl. Phys. B **586** (2000) 92 [arXiv:hep-ph/0003180], Phys. Lett. B **495** (2000) 155 [arXiv:hep-ph/0009212]; and references therein.

[17] S. Heinemeyer, W. Hollik and G. Weiglein, Comput. Phys. Commun. **124**, 76 (2000) [arXiv:hep-ph/9812320]; S. Heinemeyer, W. Hollik and G. Weiglein, Eur. Phys. J. C **9** (1999) 343 [arXiv:hep-ph/9812472].

[18] H. N. Brown *et al.* [Muon g-2 Collaboration], Phys. Rev. Lett. **86**, 2227 (2001) [arXiv:hep-ex/0102017].

[19] M. Knecht and A. Nyffeler, arXiv:hep-ph/0111058; M. Knecht, A. Nyffeler, M. Perrottet and E. De Rafael, arXiv:hep-ph/0111059; M. Hayakawa and T. Kinoshita, arXiv:hep-ph/0112102; I. Blokland, A. Czarnecki and K. Melnikov, arXiv:hep-ph/0112117; J. Bijnens, E. Pallante and J. Prades, arXiv:hep-ph/0112255.

[20] R. Alemany, M. Davier and A. Hocker, Eur. Phys. J. C **2** (1998) 123 [arXiv:hep-ph/9703220]; M. Davier and A. Hocker, Phys. Lett. B **419** (1998) 419 [arXiv:hep-ph/9711308]; M. Davier and A. Hocker, Phys. Lett. B **435** (1998) 427 [arXiv:hep-ph/9805470]; S. Narison, Phys. Lett. B **513** (2001) 53 [arXiv:hep-ph/0103199]; J. F. De Troconiz and F. J. Yndurain, arXiv:hep-ph/0106025.

[21] L. L. Everett, G. L. Kane, S. Rigolin and L. Wang, Phys. Rev. Lett. **86**, 3484 (2001) [arXiv:hep-ph/0102145]; J. L. Feng and K. T. Matchev, Phys. Rev. Lett. **86**, 3480 (2001)

[arXiv:hep-ph/0102146]; E. A. Baltz and P. Gondolo, Phys. Rev. Lett. **86**, 5004 (2001) [arXiv:hep-ph/0102147]; U. Chattopadhyay and P. Nath, Phys. Rev. Lett. **86**, 5854 (2001) [arXiv:hep-ph/0102157]; S. Komine, T. Moroi and M. Yamaguchi, Phys. Lett. B **506**, 93 (2001) [arXiv:hep-ph/0102204]; J. Ellis, D. V. Nanopoulos and K. A. Olive, Phys. Lett. B **508** (2001) 65 [arXiv:hep-ph/0102331]; R. Arnowitt, B. Dutta, B. Hu and Y. Santoso, Phys. Lett. B **505** (2001) 177 [arXiv:hep-ph/0102344] S. P. Martin and J. D. Wells, Phys. Rev. D **64**, 035003 (2001) [arXiv:hep-ph/0103067]; H. Baer, C. Balazs, J. Ferrandis and X. Tata, Phys. Rev. D **64**, 035004 (2001) [arXiv:hep-ph/0103280].

[22] S. Mizuta and M. Yamaguchi, Phys. Lett. B **298** (1993) 120 [arXiv:hep-ph/9208251]; J. Edsjo and P. Gondolo, Phys. Rev. D **56** (1997) 1879 [arXiv:hep-ph/9704361].

[23] J. Ellis, T. Falk and K. A. Olive, Phys. Lett. B **444** (1998) 367 [arXiv:hep-ph/9810360]; J. Ellis, T. Falk, K. A. Olive and M. Srednicki, Astropart. Phys. **13** (2000) 181 [arXiv:hep-ph/9905481]; M. E. Gómez, G. Lazarides and C. Pallis, Phys. Rev. D **61** (2000) 123512 [arXiv:hep-ph/9907261] and Phys. Lett. B **487** (2000) 313 [arXiv:hep-ph/0004028]; R. Arnowitt, B. Dutta and Y. Santoso, Nucl. Phys. B **606** (2001) 59 [arXiv:hep-ph/0102181].

[24] C. Boehm, A. Djouadi and M. Drees, Phys. Rev. D **62** (2000) 035012 [arXiv:hep-ph/9911496].

[25] J. Ellis, K.A. Olive and Y. Santoso, arXiv:hep-ph/0112113.

[26] M. Drees and M. M. Nojiri, Phys. Rev. D **47** (1993) 376 [arXiv:hep-ph/9207234]; H. Baer and M. Brhlik, Phys. Rev. D **53** (1996) 597 [arXiv:hep-ph/9508321] and Phys. Rev. D **57** (1998) 567 [arXiv:hep-ph/9706509]; H. Baer, M. Brhlik, M. A. Diaz, J. Ferrandis, P. Mercadante, P. Quintana and X. Tata, Phys. Rev. D **63** (2001) 015007 [arXiv:hep-ph/0005027]; A. B. Lahanas, D. V. Nanopoulos and V. C. Spanos, Mod. Phys. Lett. A **16** (2001) 1229 [arXiv:hep-ph/0009065].

[27] J. L. Feng, K. T. Matchev and T. Moroi, Phys. Rev. Lett. **84**, 2322 (2000) [arXiv:hep-ph/9908309]; J. L. Feng, K. T. Matchev and T. Moroi, Phys. Rev. D **61**, 075005 (2000) [arXiv:hep-ph/9909334]; J. L. Feng, K. T. Matchev and F. Wilczek, Phys. Lett. B **482**, 388 (2000) [arXiv:hep-ph/0004043].

[28] J. R. Ellis and K. A. Olive, Phys. Lett. B **514** (2001) 114 [arXiv:hep-ph/0105004].

[29] For other recent calculations, see, for example: A. B. Lahanas, D. V. Nanopoulos and V. C. Spanos, Phys. Lett. B **518** (2001) 94 [arXiv:hep-ph/0107151]; V. Barger and C. Kao, Phys. Lett. B **518**, 117 (2001) [arXiv:hep-ph/0106189]; L. Roszkowski, R. Ruiz de Austri and T. Nihei, JHEP **0108**, 024 (2001) [arXiv:hep-ph/0106334]; A. Djouadi, M. Drees and J. L. Kneur, JHEP **0108**, 055 (2001) [arXiv:hep-ph/0107316].

[30] J. Ellis, K. Enqvist, D. V. Nanopoulos and F. Zwirner, Mod. Phys. Lett. A **1**, 57 (1986); R. Barbieri and G. F. Giudice, Nucl. Phys. B **306** (1988) 63.

[31] See, for example: I. Hinchliffe, F. E. Paige, M. D. Shapiro, J. Soderqvist and W. Yao, Phys. Rev. D **55** (1997) 5520; TESLA Technical Design Report, DESY-01-011, Part III, *Physics at an $e^+e^-$ Linear Collider* (March 2001).

[32] M. Battaglia *et al.*, Eur. Phys. J. C **22** (2001) 535 [arXiv:hep-ph/0106204].

[33] ATLAS Collaboration, *ATLAS detector and physics performance Technical Design Report*, CERN/LHCC 99-14/15 (1999); S. Abdullin *et al.* [CMS Collaboration], arXiv:hep-ph/9806366; S. Abdullin and F. Charles, Nucl. Phys. B **547** (1999) 60 [arXiv:hep-ph/9811402]; CMS Collaboration, Technical Proposal, CERN/LHCC 94-38 (1994).

[34] M. Battaglia *et al.*, in *Proc. of the APS/DPF/DPB Summer Study on the Future of Particle Physics (Snowmass 2001)* , eds. R. Davidson and C. Quigg, arXiv:hep-ph/0112013.

[35] S. Matsumoto *et al.* [JLC Group], *JLC-1*, KEK Report 92-16 (1992); J. Bagger *et al.* [American Linear Collider Working Group], *The Case for a 500-GeV $e^+e^-$ Linear Collider*, SLAC-PUB-8495, BNL-67545, FERMILAB-PUB-00-152, LBNL-46299, UCRL-ID-139524, LBL-46299, Jul 2000, arXiv:hep-ex/0007022; T. Abe *et al.* [American Linear Collider Working Group Collaboration], *Linear Collider Physics Resource Book for Snowmass 2001*, SLAC-570, arXiv:hep-ex/0106055, hep-ex/0106056, hep-ex/0106057 and hep-ex/0106058; TESLA Technical Design Report, DESY-01-011, Part III, *Physics at an $e^+e^-$ Linear Collider* (March 2001).

[36] R. W. Assmann *et al.* [CLIC Study Team], *A 3-TeV $e^+e^-$ Linear Collider Based on CLIC Technology*, ed. G. Guignard, CERN 2000-08; CLIC Physics Study Group, `http://clicphysics.web.cern.ch/CLICphysics/`.

[37] Neutrino Factory and Muon Collider Collaboration,
`http://www.cap.bnl.gov/mumu/ mu_home_page.html`;
European Muon Working Groups,
`http://muonstoragerings.cern.ch/Welcome.html`.

[38] G. A. Blair, W. Porod and P. M. Zerwas, Phys. Rev. **D63** (2001) 017703 [arXiv:hep-ph/0007107].

[39] J. Ellis, J. L. Feng, A. Ferstl, K. T. Matchev and K. A. Olive, arXiv:astro-ph/0110225.

[40] CDMS Collaboration, R. W. Schnee *et al.*, Phys. Rept. **307**, 283 (1998).

[41] CRESST Collaboration, M. Bravin *et al.*, Astropart. Phys. **12**, 107 (1999) [arXiv:hep-ex/9904005].

[42] H. V. Klapdor-Kleingrothaus, arXiv:hep-ph/0104028.

[43] DAMA Collaboration, R. Bernabei *et al.*, Phys. Lett. B **436** (1998) 379.

[44] G. Jungman, M. Kamionkowski and K. Griest, Phys. Rept. **267**, 195 (1996) [arXiv:hep-ph/9506380]; `http://t8web.lanl.gov/people/jungman/neut-package.html`.

[45] H. Murayama and A. Pierce, arXiv:hep-ph/0108104.

[46] J. R. Ellis, J. S. Hagelin, S. Kelley and D. V. Nanopoulos, Nucl. Phys. B **311** (1988) 1.

[47] C. K. Jung, arXiv:hep-ex/0005046; Y. Suzuki *et al.* [TITAND Working Group Collaboration], arXiv:hep-ex/0110005.